Journal of Physics:
Conference Series

PAPER • OPEN ACCESS

Modeling of underwater vehicle positioning accuracy assessment based on ultrashort baseline

To cite this article: Zizhuo Liu *et al* 2025 *J. Phys.: Conf. Ser.* **2996** 012016

Modeling of underwater vehicle positioning accuracy assessment based on ultrashort baseline

Zizhuo Liu[1*], Chengming Luo[1], Hongxuan Fan[1], Zicheng Dou[1] and Han Xu[2]

[1]Ocean College, Jiangsu University of Science and Technology, Zhenjiang, 212003, China
[2]Tongji Zhejiang College, Jiaxing 314000, China

[*]Corresponding author's e-mail: liuzizhuo074@163.com

Abstract. Considering the effects of complexity and uncertainty in underwater environments, solving the lower bound of the underwater vehicle positioning error variance is crucial for assessing positioning accuracy. To address the problem of nonlinear measurement equations for underwater acoustic sensors with ultrashort baseline measurements of underwater vehicles, this paper designs a method for recursively deriving an improved posterior Cramer-Rao lower bound for underwater vehicles using Taylor expansion linearization and then conducts simulation experiments. The results show that the improved posterior Cramer-Rao lower bound has good results and can be used as an evaluation standard for the positional results of underwater vehicle filter estimates.

1. Introduction

Underwater vehicle is a kind of underwater equipment integrating the functions of power propulsion, multi-sensor fusion, navigation, and communication as well as computer control, etc., which can move freely in the underwater three-dimensional space, it is one of the main platforms for human beings to explore and develop the oceans [1]. Navigation is one of the key challenges faced by underwater vehicles, and the ability of underwater vehicle navigation to provide accurate position, velocity, and attitude information determines whether or not an underwater vehicle can move to a predetermined location according to a predetermined route and return home safely [2]. Underwater acoustic signals are able to travel longer distances compared to electromagnetic signals, so acoustic navigation is also an important means of navigation for underwater vehicles [3]. The overall structure of acoustic navigation for underwater vehicles mainly includes the base array, transponder, and ground station. Among them, the base array is a set of arrays capable of acoustic-electric signal conversion, and the position of each array element has been accurately determined. The transponder equipped with transducers is capable of responding to signals in specific frequency bands and forms. The ground station consists of components such as network switches, data memories, data processing systems, and human-machine interaction platforms [4]. According to the length of the baseline hydroacoustic positioning can be divided into Long Base Line, Short Base Line, and Ultrashort Baseline.

Although underwater vehicle acoustic navigation has become a major means, there are uncertainties such as underwater target maneuvering operation, unknown complex environments, etc. At the same time, various interferences such as marine environmental noise, marine biological noise ships, etc., are prone to cause hydroacoustic measurements of the noise wild value thus seriously reducing the navigation accuracy of the underwater vehicle. Aiming at the problem of uncertainty in the reference coordinates of underwater sensors in extreme environments, Liu et al. derived the extended Cramer-Rao lower bound equations based on the arrival time difference of underwater multipath channels [5]. The problem of large noise caused by multiple uncertain measurements underwater has also been considered, and a lower bound on the variance under mixed measurements has been given by combining the time difference of arrival and azimuth of angle [6]. Aiming at the problem that the slow propagation speed of

Journal of Physics: Conference Series **2996** (2025) 012016 doi:10.1088/1742-6596/2996/1/012016

hydroacoustic signals leads to the Doppler effect affecting the localization accuracy, some scholars have also investigated the lower bound of the variance under the hydroacoustic sound velocity bending and the base array calibration error and evaluated the measurement parameters under the Doppler effect [7]. Aiming at the underwater localization which is easily affected by the harsh environment leading to the uncertainty of the deployed position of the hydroacoustic base array, Saeed et al. derived closed-form expressions for the Cramer-Rao lower bound under the time of arrival and angle of arrival measurements, and analyzed the localization accuracy of underwater robots under the uncertain node coordinates [8]. In this paper, an ultrashort baseline system hydroacoustic sensor measurement is used to establish the nonlinear measurement equation of the underwater vehicle, while Taylor's first-order expansion linearizes the nonlinear measurement equation, which in turn leads to the derivation of the improved posterior Cramer-Rao lower bound.

2. Underwater vehicle motion modeling

Assuming that the underwater vehicle is in uniform circular motion underwater, its equation of state is modeled as:

$$\mathbf{x}_{k+1} = \mathbf{F}_k \mathbf{x}_k + \mathbf{G}_k \mathbf{w}_k \tag{1}$$

where $\mathbf{x}_k = [x_k, \dot{x}_k, y_k, \dot{y}_k]'$ is the position and velocity of the underwater vehicle in the two-dimensional direction, the state transfer matrix is $\mathbf{F}_k = \begin{bmatrix} 1 & \frac{\sin(\omega T)}{\omega} & 0 & -\frac{1-\cos(\omega T)}{\omega} \\ 0 & \cos(\omega T) & 0 & -\sin(\omega T) \\ 0 & \frac{1-\cos(\omega T)}{\omega} & 1 & \frac{\sin(\omega T)}{\omega} \\ 0 & \sin(\omega T) & 0 & \cos(\omega T) \end{bmatrix}$, the noise driver matrix is $\mathbf{G}_k = \begin{bmatrix} T^2/2 & 0 \\ T & 0 \\ 0 & T^2/2 \\ 0 & T \end{bmatrix}$, $\mathbf{w}_k$ is a Gaussian noise with mean $\mathbf{0}$ and variance $\mathbf{Q}_k$.

Based on the horizontal azimuth θ_k and distance d_k between the base station and the underwater vehicle measured by the hydroacoustic sensor, the measurement equation is established as:

$$\mathbf{z}_k = h(\mathbf{x}_k) + \mathbf{v}_k \tag{2}$$

$$h(\mathbf{x}_k) = \begin{bmatrix} \arctan\left(\dfrac{y_k - y_0}{x_k - x_0}\right) \\ \sqrt{(x_k - x_0)^2 + (y_k - y_0)^2} \end{bmatrix} \tag{3}$$

where $\mathbf{z}_k = [\theta_k, d_k]'$, $\mathbf{v}_k$ is Gaussian noise with mean $\mathbf{0}$ and variance $\mathbf{R}_k$, assuming that the process noise $\mathbf{w}_k$ and the measurement noise $\mathbf{v}_k$ are uncorrelated, $[x_0, y_0]'$ is the location of the base station.

3. Improved posterior Cramer-Rao lower bound derivation

The Fisher information matrix needs to be derived from the underwater vehicle state probability density function, Based on the established underwater vehicle state equations and measurement equations, the underwater vehicle expectation and variance can be obtained to derive its improved posterior Cramer-Rao lower bound (IPCRLB). Since the state equations are linear equations, the expectation and variance of the target at the next moment can be derived from the state at the previous moment, while the established measurement equations for the underwater vehicle are nonlinear equations, which need to linearize the nonlinear equations and derive the target expectation and variance.

Journal of Physics: Conference Series **2996** (2025) 012016 doi:10.1088/1742-6596/2996/1/012016

The state of the underwater vehicle at moment k is estimated to be $\hat{\mathbf{x}}_k$, and the target state at moment k+1 is obtained from the state equation as:

$$\hat{\mathbf{x}}_{k+1|k} = \mathbf{F}_k \hat{\mathbf{x}}_k + \mathbf{G}\mathbf{w}_k \tag{4}$$

The state expectation of the underwater vehicle at the moment k+1 is:

$$\mu_{k+1}^f = E\left[\mathbf{x}_{k+1}\right] = E\left[\mathbf{F}_k \mathbf{x}_k + \mathbf{G}_k \mathbf{w}_k\right] \tag{5}$$

where $\mathbf{F}_k \mathbf{x}_k$ is a linear equation, according to the additive and linear nature of the expectation:

$$E\left[\mathbf{F}_k \mathbf{x}_k + \mathbf{G}_k \mathbf{w}_k\right] = E\left[\mathbf{F}_k \mathbf{x}_k\right] + E\left[\mathbf{G}_k \mathbf{w}_k\right] = \mathbf{F}_k E\left[\mathbf{x}_k\right] + \mathbf{G}_k E\left[\mathbf{w}_k\right] \tag{6}$$

where $E\left[\mathbf{x}_k\right] = \hat{\mathbf{x}}_k$, $E\left[\mathbf{w}_k\right] = 0$.

Therefore the underwater vehicle state expectation at time k+1 is denoted as:

$$\mu_{k+1}^f = \mathbf{F}_k \hat{\mathbf{x}}_k \tag{7}$$

The error between $\mathbf{x}_{k+1}$ and its mean is expected to obtain the state variance of the underwater vehicle at moment k+1, where the error between $\mathbf{x}_{k+1}$ and its mean is denoted as:

$$\tilde{\mathbf{x}}_{k+1} = \mathbf{x}_{k+1} - \mu_{k+1}^f = \mathbf{F}_k\left(\mathbf{x}_k - \hat{\mathbf{x}}_k\right) + \mathbf{G}_k \mathbf{w}_k \tag{8}$$

The expression for the variance is:

$$\mathbf{C}_{k+1}^f = E\left[\tilde{\mathbf{x}}_{k+1}\tilde{\mathbf{x}}_{k+1}'\right] = \mathbf{F}_k \hat{\mathbf{P}}_k^f \mathbf{F}_k + \mathbf{G}_k \mathbf{Q}_k \mathbf{G}_k' \tag{9}$$

Thus the underwater vehicle state at moment k+1 obeys a Gaussian distribution of:

$$\mathbf{x}_{k+1} \sim \mathcal{N}\left[\mathbf{x}_{k+1}; \mu_{k+1}^f, C_{k+1}^f\right] \tag{10}$$

The measurement equations of the established underwater vehicle are nonlinear and are linearized by a first-order Taylor expansion of the measurement equations:

$$\mathbf{z}_{k+1} \approx h\left(\hat{\mathbf{x}}_{k+1|k}\right) + \boldsymbol{F}_{k+1}^h\left(\hat{\mathbf{x}}_{k+1|k}\right)\tilde{\mathbf{x}}_{k+1} + \mathbf{v}_{k+1} \tag{11}$$

where $\boldsymbol{F}_{k+1}^h\left(\hat{\mathbf{x}}_{k+1|k}\right) = \left(\dfrac{\partial h^{\boldsymbol{T}}\left(\mathbf{x}_{k+1}\right)}{\partial \mathbf{x}_{k+1}}\right)^{\boldsymbol{T}}\Bigg|_{\mathbf{x}_{k+1}=\hat{\mathbf{x}}_{k+1|k}}$, the predicted state error $\tilde{\mathbf{x}}_{k+1} = \mathbf{x}_{k+1} - \hat{\mathbf{x}}_{k+1|k}$.

The expectation of the underwater vehicle measurement state is:

$$\mu_{k+1}^h = E\left[\mathbf{z}_{k+1}\right] = h\left(\hat{\mathbf{x}}_{k+1|k}\right) + \boldsymbol{F}_{k+1}^h\left(\hat{\mathbf{x}}_{k+1|k}\right)E\left[\tilde{\mathbf{x}}_{k+1}\right] \tag{12}$$

where $E\left[\tilde{\mathbf{x}}_{k+1}\right] = 0$, the mean value of $\mathbf{v}_{k+1}$ is $\mathbf{0}$, so the mean value of the predicted measurement state is denoted as:

$$\mu_{k+1}^h = h\left(\hat{\mathbf{x}}_{k+1|k}\right) \tag{13}$$

The prediction error of the measured state at k+1 moments is:

$$\tilde{\mathbf{z}}_{k+1} = \mathbf{z}_{k+1} - \mu_{k+1}^h = \boldsymbol{F}_{k+1}^h\left(\hat{\mathbf{x}}_{k+1|k}\right)\tilde{\mathbf{x}}_{k+1} + \mathbf{v}_{k+1} \tag{14}$$

Squaring the expectation of the prediction error yields the variance of the predicted measurement state of the underwater vehicle:

$$C_{k+1}^h = E\left[\tilde{\mathbf{z}}_{k+1}\tilde{\mathbf{z}}_{k+1}'\right] \approx \boldsymbol{F}_{k+1}^h\left(\hat{\mathbf{x}}_{k+1|k}\right)\hat{P}_{k+1}^h \boldsymbol{F}_{k+1}^h\left(\hat{\mathbf{x}}_{k+1|k}\right)' + \mathbf{R}_{k+1} \tag{15}$$

where $\hat{P}_{k+1}^h = E\left[\left(\mathbf{x}_{k+1} - \hat{\mathbf{x}}_{k+1|k}\right)\left(\mathbf{x}_{k+1} - \hat{\mathbf{x}}_{k+1|k}\right)'\right]$.

Therefore the measured state of the underwater vehicle at k+1 moments obeys a Gaussian distribution as:

$$\mathbf{z}_{k+1} \sim \mathcal{N}\left[\mathbf{z}_{k+1}; \mu_{k+1}^h, C_{k+1}^h\right] \tag{16}$$

The recursive formula for the PCRLB is:

$$\mathbf{J}_{k+1} = \mathbf{D}_{k+1}^{22} - \mathbf{D}_k^{21}(\mathbf{J}_k + \mathbf{D}_k^{11})^{-1}\mathbf{D}_k^{12} \quad (k>0) \tag{17}$$

$$\mathbf{D}_k^{11} = \mathrm{E}\left[(\nabla_{\mathbf{x}_k} \log p(\mathbf{x}_{k+1}|\mathbf{x}_k))(\nabla_{\mathbf{x}_k} \log p(\mathbf{x}_{k+1}|\mathbf{x}_k))'\right] \tag{18}$$

Journal of Physics: Conference Series **2996** (2025) 012016 doi:10.1088/1742-6596/2996/1/012016

$$\mathbf{D}_k^{12} = \mathrm{E}\left[(\nabla_{\mathbf{x}_k} \log p(\mathbf{x}_{k+1}|\mathbf{x}_k))(\nabla_{\mathbf{x}_{k+1}} \log p(\mathbf{x}_{k+1}|\mathbf{x}_k))'\right] \tag{19}$$

$$\mathbf{D}_k^{21} = (\mathbf{D}_k^{12})^T \tag{20}$$

$$\begin{aligned}\mathbf{D}_{k+1}^{22} &= \mathrm{E}\left[(\nabla_{\mathbf{x}_{k+1}} \log p(\mathbf{x}_{k+1}|\mathbf{x}_k))(\nabla_{\mathbf{x}_{k+1}} \log p(\mathbf{x}_{k+1}|\mathbf{x}_k))'\right] \\ &+\mathrm{E}\left[(\nabla_{\mathbf{x}_{k+1}} \log p(\mathbf{z}_{k+1}|\mathbf{x}_{k+1}))(\nabla_{\mathbf{x}_{k+1}} \log p(\mathbf{z}_{k+1}|\mathbf{x}_{k+1}))'\right]\end{aligned} \tag{21}$$

Based on the derived Gaussian distribution that the underwater vehicle states and measurements obey, the probability density function is:

$$\begin{aligned}&p\left(\mathbf{x}_{k+1}|\mathbf{x}_k\right) \\ &= \frac{1}{\sqrt{(2\pi)^4 \det\left(C_{k+1}^f\right)}} \exp\left[-\frac{1}{2}\left(\mathbf{x}_{k+1} - \mu_{k+1}^f\right)' \left(C_{k+1}^f\right)^{-1} \left(\mathbf{x}_{k+1} - \mu_{k+1}^f\right)\right]\end{aligned} \tag{22}$$

$$\begin{aligned}&p\left(\mathbf{z}_{k+1}|\mathbf{x}_{k+1}\right) \\ &= \frac{1}{\sqrt{(2\pi)^2 \det\left(C_{k+1}^h\right)}} \exp\left[-\frac{1}{2}\left(\mathbf{z}_{k+1} - \mu_{k+1}^h\right)^T \left(C_{k+1}^h(\mathbf{x}_{k+1})\right)^{-1} \left(\mathbf{z}_{k+1} - \mu_{k+1}^h\right)\right]\end{aligned} \tag{23}$$

$$\begin{aligned}&\nabla_{\mathbf{x}_k}\left[\ln p\left(\mathbf{x}_{k+1}|\mathbf{x}_k\right)\right] \\ &= -\frac{1}{2}\frac{\partial \ln\det C_{k+1}^f}{\partial \mathbf{x}_k} - \frac{1}{2}\frac{\partial\left[\left(\mathbf{x}_{k+1} - \mu_{k+1}^f\right)' \left(C_{k+1}^f\right)^{-1} \left(\mathbf{x}_{k+1} - \mu_{k+1}^f\right)\right]}{\partial \mathbf{x}_k}\end{aligned} \tag{24}$$

$$\nabla_{\mathbf{x}_{k+1}}\left[\ln p\left(\mathbf{x}_{k+1}|\mathbf{x}_k\right)\right] = -\left(C_{k+1}^f\right)^{-1}\left(\mathbf{x}_{k+1} - \mu_{k+1}^f\right) \tag{25}$$

$$\begin{aligned}&\nabla_{\mathbf{x}_{k+1}}\left[\ln p\left(\mathbf{z}_{k+1}|\mathbf{x}_{k+1}\right)\right] \\ &= -\frac{1}{2}\frac{\partial \ln\det C_{k+1}^h}{\partial \mathbf{x}_{k+1}} - \frac{1}{2}\frac{\partial\left[\left(\mathbf{z}_{k+1} - \mu_{k+1}^h\right)' \left(C_{k+1}^h\right)^{-1} \left(\mathbf{z}_{k+1} - \mu_{k+1}^h\right)\right]}{\partial \mathbf{x}_{k+1}}\end{aligned} \tag{26}$$

Substituting Equations (24), (25), and (26) into the recursive formula yields the Fisher information matrix, which is inverted to obtain the IPCRLB for the underwater vehicle, the IPCRLB for the position of the underwater vehicle in the x-direction is $\sqrt{\mathbf{J}_{k+1}^{-1}(1,1)}$, the IPCRLB for the position of the underwater vehicle in the y-direction is $\sqrt{\mathbf{J}_{k+1}^{-1}(3,3)}$.

4. Simulation

The experimental environment for this simulation is MatlabR2021, the base station position is set to $[0,0]'$, the position and velocity of the underwater vehicle in each direction of the initial state are set to $[100,10,100,10]'$, the process noise covariance matrix $\mathbf{Q}_k = diag\left[0.01^2\ 0.01^2\right]$, the measurement noise covariance matrix $\mathbf{R}_k = diag\left[0.01^2\ 1^2\right]$, the simulation is set to run the underwater vehicle for 250s, the sampling interval is 1s, the number of particles is 100, and 50 Monte Carlo simulations are performed. The KF, UKF, and MPF estimation results are compared with the IPCRLB proposed in this paper. Figure 1 shows the horizontal direction motion trajectory of the underwater vehicle.

Figure 2 shows the position error of KF, UKF, MPF, and IPCRLB proposed in this paper in x and y directions, respectively, according to the simulation results we can get that the position errors of KF, UKF, MPF, and IPCRLB in the x-direction are 4.94, 1.94, 0.97, and 0.70m, respectively, the position errors in the y-direction are 4.71, 1.55, 0.93, and 0.20 m, The overall position errors of the IPCRLB proposed in this paper are lower than the filtered estimation result errors in both x and y directions, which can be used as an evaluation standard for the filtered estimation.

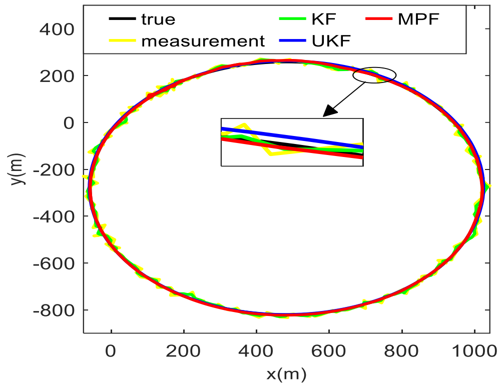

Figure 1. Underwater vehicle trajectory.

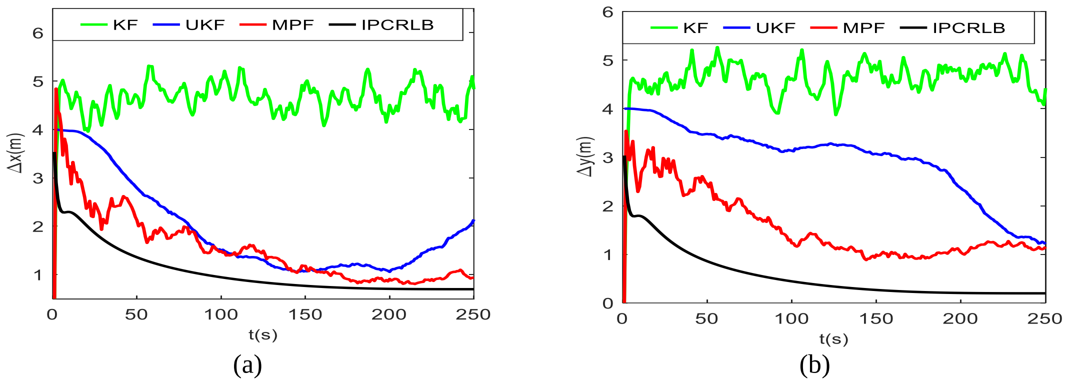

Figure 2. Position error in x and y directions.

In order to better analyze and compare the IPCRLB with different filtering algorithm errors, the overall positional error curves are plotted as shown in Figure 3. According to Figure 3, the overall position errors of KF, UKF, MPF, and IPCRLB obtained from the simulation are 6.60, 2.48, 1.35, and 0.90 m, respectively. The overall position error trend is consistent with the position error trend in each direction, and the IPCRLB as a whole is located below each filter result, which can be used as a standard for underwater vehicle position estimation error assessment.

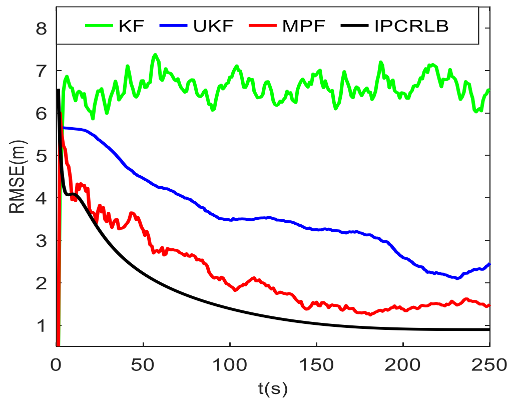

Figure 3. Total position error.

5. Conclusion

Considering the nonlinear problem of underwater vehicle measurement equations established based on hydroacoustic sensor measurements, this paper linearizes the nonlinear measurement equations with

Taylor's first-order expansion, solves the problem of recursive state expectation and variance under the nonlinear equations, and derives IPCRLB. The simulation results show that the IPCRLB derived from the Taylor expansion linearized measurement equation is lower than the filtering estimation error and can be used as an evaluation criterion with high practical value.

Acknowledgments

This work was financially supported by the National Natural Science Foundation of China (62001195, 52071164, 42204126), Jiangsu Qinglan Project, and the Development Fund of Jiangsu Key Laboratory of Power Transmission & Distribution Equipment Technology (2023JSSPD10), and by the Science and Technology Plan Project of Jiaxing under Grant 2023AZ31008, by the General Scientific Research Project of the Zhejiang Provincial Department of Education under Grant Y202250228.

References

[1] Christopher V A (2003) Autonomous underwater vehicles: Autonomous Underwater Lagrangian Platform and Sensors., pp. 1-5.
[2] Yan J, Guo Z W, Yang X, Luo X Y and Guan X P (2022) Finite-time tracking control of the autonomous underwater vehicle without velocity measurements. IEEE Transactions on Systems Man Cybernetics-Systems., 52(11): 6759-6773.
[3] McCarthy A, Sen Gupta A and Hawk E (2020) Support-constrained mixed-norm optimization techniques for estimating multipath activity in shallow water acoustic channels. IEEE Journal of Oceanic Engineering., 45(3): 683-698.
[4] Huang H, Zheng Y R (2018) Node localization with AoA assistance in multi-hop underwater sensor networks. AD Hoc Networks., 78:32-41.
[5] Liu Y, Wang Y M, and Chen C (2023) Efficient underwater acoustical localization method based on TDOA with sensor position errors. Journal of Marine Science and Engineering., 11(4): 861.
[6] Zhang L, Zhang T, Shin H S, et al. (2021) Efficient underwater acoustical localization method based on time difference and bearing measurements. IEEE Transactions on Instrumentation and Measurement., 70: 1-16.
[7] Zhang B B, Hu Y C, Wang H Y, et al. (2018) Underwater source localization using TDOA and FDOA measurements with unknown propagation speed and sensor parameter errors. IEEE Access., 6: 36645-36661.
[8] Saeed N, Celik A, Alouini M S, et al. (2020) Analysis of 3D localization in underwater optical wireless networks with uncertain anchor positions. Science China-Information Sciences., 63(10): 202305.